Time-based Chern number in periodically driven systems in the adiabatic limit

I-Te Lu,[1] Dongbin Shin,[1,2] Umberto De Giovannini,[1,3] Hannes Hübener,[1] Jin Zhang,[1] Simone Latini,[1,4] and Angel Rubio[1,5,*]

[1]*Max Planck Institute for the Structure and Dynamics of Matter and Center for Free-Electron Laser Science, Luruper Chaussee 149, Hamburg 22761, Germany*

[2]*Department of Physics and Photon Science, Gwangju Institute of Science and Technology (GIST), Gwangju 61005, Republic of Korea*

[3]*Università degli Studi di Palermo, Dipartimento di Fisica e Chimica-Emilio Segré, Palermo I-90123, Italy*

[4]*Department of Physics, Technical University of Denmark, 2800 Kgs. Lyngby, Denmark*

[5]*Center for Computational Quantum Physics (CCQ), The Flatiron Institute, 162 Fifth avenue, New York, NewYork 10010, United States of America*

(Received 14 September 2022; revised 3 January 2023; accepted 18 January 2023; published 6 February 2023)

To define the topology of driven systems, recent works have proposed synthetic dimensions as a way to uncover the underlying parameter space of topological invariants. Using time as a synthetic dimension, together with a momentum dimension, gives access to a *synthetic* two-dimensional (2D) Chern number. It is, however, still unclear how the synthetic 2D Chern number is related to the Chern number that is defined from a parametric variable that evolves with time. Here we show that in periodically driven systems in the *adiabatic limit*, the synthetic 2D Chern number is a multiple of the Chern number defined from the parametric variable. The synthetic 2D Chern number can thus be engineered via how the parametric variable evolves in its own space. We justify our claims by investigating Thouless pumping in two one-dimensional (1D) tight-binding models, a three-site chain model, and a two-1D-sliding-chains model. The present findings could be extended to higher dimensions and other periodically driven configurations.

DOI: 10.1103/PhysRevResearch.5.013081

I. INTRODUCTION

Periodically-driven quantum systems under an external time-dependent driving source have emerged as a platform for generating new exotic matter states in a wide range of materials such as atomic gases, two-dimensional (2D), twisted, and bulk materials [1–5]. These systems can be interpreted in terms of quasiparticles that are modified or dressed by the harmonics of external driving sources from low to high frequencies [2,6,7]. The quasiparticles band structures can in turn be classified by the band topological invariants [4].

The 2D Chern number, a topological invariant on a closed surface, is usually evaluated in the space-related dimensions, e.g., Brillouin zone, of solid state materials, which are limited at most to the three-dimensional (3D) spatial space. To extend the classification to dimensions other than spatial dimensions, the so-called synthetic (nonspatial) dimensions have been proposed to expand the concepts of topology to higher dimensions, opening a new way to design materials properties [8–13].

For periodically-driven systems, one of the relevant synthetic dimensions is the Floquet frequencies of an external driving; based on the topological invariants of the synthetic dimensions, a number of interesting physical phenomena such as quantized energy exchange between the external driving fields have been predicted [14–18]. In contrast to such a dimension formed by the Floquet frequencies, using time itself directly as a synthetic dimension is somewhat less intuitive, and this is what we are going to explore in the present work.

Indeed, causality sets that we cannot move backward in time to define a closed loop in parameter space that is needed when computing a 2D Chern number that involves the time dimension. Nevertheless, time has been used as a synthetic dimension, together with the momentum dimension, to compute a 2D Chern number for a time- and spatially-periodic Hamiltonian $H(t+T, x+a) = H(t, x)$, where t is time, T the time period, x the spatial coordinate, and a the lattice constant [19]. In such cases, the Chern number represents the number of pumped quantum charges, known as Thouless (or quantum) pumping [20], which has been demonstrated in many different experiments [19,21,22].

In this work we reveal that in a periodically driven system, even though the time dependence is parametric, the *synthetic* 2D Chern number–obtained using time as one of the two dimensions–can be built upon another Chern number defined on the parametric dimension α, which evolves with time and can define a loop in its parameter space, e.g., the position of the nuclei in a solid, the vector potential of an external field, etc. We provide an analytical proof that, in the *adiabatic limit* the 2D Chern number $C^{\{t\text{-}k\}}$, which involves the time t dimension and a spatial (momentum) k dimension, is always an integer multiple of another, more fundamental 2D Chern number $C^{\{\alpha\text{-}k\}}$, which involves a periodic parametric function $\alpha(t)$

*angel.rubio@mpsd.mpg.de

that follows $\alpha(t+T)=\alpha(t)+l$ where l is an integer. This integer multiple can thus be used to classify a periodically-driven system in the adiabatic limit. Our finding suggests that the proposed synthetic 2D Chern number $C^{\{t\text{-}k\}}$ can be designed via the trajectory of the parametric variable $\alpha(t)$.

II. TIME AS A SYNTHETIC DIMENSION

For the sake of simplicity and without loss of generality, suppose we have a one-dimensional (1D) real-space periodic Hamiltonian $H(\alpha, x+a)=H(\alpha,x)$ with a tuning time-dependent parameter $\alpha(t)$; here a is set to 2π below without loss of generality. It is convenient to transform the Hamiltonian to the momentum space $H(\alpha,k)$, with the crystal momentum k in the first Brillouin zone. Starting from such Hamiltonian, we make the following assumptions. The Hamiltonian is periodic in the α parametric space $H(\alpha+1,k)=H(\alpha,k)$; we are allowed to do so as α can always be conveniently rescaled. We further assume that no gap closure occurs–adiabatic approximation–for any value of α, enabling us to compute the Chern number later; we will address the interesting case of gap closing in a follow up work. For a given α value, the eigenstates for the Hamiltonian $H(\alpha,k)$ are the Bloch waves with a band index n, $|u_n(\alpha,k)\rangle$. Below we use the periodic gauge for the Bloch wave functions, i.e., $|u_n(\alpha,k+1)\rangle=|u_n(\alpha,k)\rangle$ [23]. The Chern number for the Bloch wave function with band index n on the $\alpha-k$ plane is computed using the standard definition [23]: $C_n^{\{\alpha\text{-}k\}}=\frac{1}{2\pi}\iint_{S_{\alpha k}}\Omega_{n,\alpha k}\,d\alpha dk$, where the integration is over the 2D closed surface $S_{\alpha k}$ formed by the two dimensions, α and k. The Berry curvature is then defined as $\Omega_{n,\alpha k}=\partial_\alpha A_{n,k}-\partial_k A_{n,\alpha}$, where $\partial_\alpha=\partial/\partial\alpha$, $\partial_k=\partial/\partial k$, and the Berry connection $A_{n,\alpha/k}=\langle u_n(\alpha,k)|\partial_{\alpha/k}|u_n(\alpha,k)\rangle$.

Now we explicitly consider the time periodicity in the Hamiltonian $H(t+T)=H(t)$ under the assumption that the time-dependent change is adiabatic at each time. To make sure that the Hamiltonian is invariant after one T period, the path of the parametric variable $\alpha(t)$ must satisfy $\alpha(t+T)=\alpha(t)+l$, where l is an integer, such that $H[\alpha(t+T)]=H[\alpha(t)+l]=H[\alpha(t)]$. Here we state our main result: The Chern number on the t-k plane, $C_n^{\{t\text{-}k\}}$, is a multiple of that evaluated on the α-k plane, i.e., $C_n^{\{t\text{-}k\}}=lC_n^{\{\alpha\text{-}k\}}$. The implications of the connection between the two invariants are as follows: (i) a periodically-driven Hamiltonian in the adiabatic limit can be categorized into different groups based on the integer l; (ii) the Chern number on the α-k plane, $C_n^{\{\alpha\text{-}k\}}$, forms the building block for the Chern number on the t-k plane, $C_n^{\{t\text{-}k\}}$ [24]. The physical meaning of the integer l is how many copies of the Chern number $C_n^{\{\alpha\text{-}k\}}$ the trajectory $\alpha(t)$ picks up within a time period.

Here we prove the above statement as follows:

$$\begin{aligned}C_n^{\{t\text{-}k\}}&=\frac{1}{2\pi}\int_0^T dt\int_0^1 dk\;\Omega_{n,tk}=\frac{1}{2\pi}\int_0^T dt\int_0^1 dk\;\partial_t A_{n,k}\\&=\frac{1}{2\pi}\int_0^T dt\;\partial_t\left(\int_0^1 dk\;A_{n,k}\right)=\frac{1}{2\pi}\int_0^T dt\;\partial_t\phi_n^{(k)}\\&=\frac{1}{2\pi}\int_{\alpha(0)}^{\alpha(T)}d\alpha\;\partial_\alpha\phi_n^{(k)}\\&=l\times\left[\frac{1}{2\pi}\int_{\alpha(0)}^{\alpha(0)+1}d\alpha\;\partial_\alpha\phi_n^{(k)}\right]=lC_n^{\{\alpha\text{-}k\}}.\end{aligned}\tag{1}$$

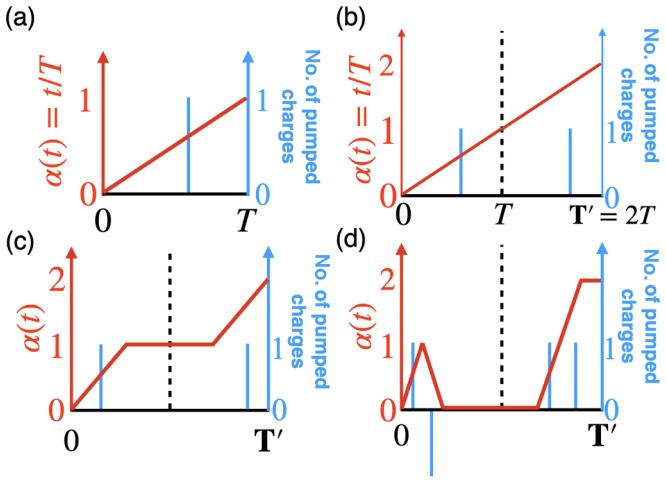

FIG. 1. Schematic illustration of the formula $C_n^{\{t\text{-}k\}}=lC_n^{\{\alpha\text{-}k\}}$. (a) The path for the parametric variable $\alpha(t)=t/T$ where T is the period. (b) The extension of (a) with a newly defined period $T'=2T$. (c) and (d) Two deformed parametric paths and the corresponding number of pumped charges as a function of time within the new time period T'.

For the last equality in the first line, the integration of $\partial_k A_t$ over the k coordinate vanishes due to the periodic gauge for the Bloch wave function. At the end of the second line, we define the Berry phase along the k coordinate as $\phi_n^{(k)}$. In the third line, we change the variable from t to α. In the last line, the integration interval $[\alpha(0),\alpha(0)+l]$ can be exactly separated into l intervals, i.e., $[\alpha(0),\alpha(0)+1]$,..., $[\alpha(0)+l-1,\alpha(0)+l]$, for each of which the Chern number $C_n^{\{\alpha\text{-}k\}}$ is the same. In 1D, the Berry phase $\phi_n^{(k)}$ is related to the center of the Wannier function via the formula $a\phi_n^{(k)}/2\pi$ [23]. The center can be regarded as the position of the charge, which may move after *one parametric loop*, i.e., quantum pumping. The number of pumped charges is equal to the Chern number $C_n^{\{\alpha\text{-}k\}}$ obtained on the $\alpha-k$ plane.

With the general concept of quantum pumping in mind, Fig. 1 provides a conceptual illustration of the implications of Eq. (1) and the meaning of the integer l. We chose $\alpha(t)=t/T$ such that the time dimension is equivalent to the parametric dimension. Figure 1(a) shows the parametric variable and the number of pumped charges as a function of time, assuming a Chern number $C^{\{\alpha\text{-}k\}}=C^{\{T\text{-}k\}}=1$; that is, the number of pumped charges is $+1$ when α goes from 0 to 1, while -1 along the opposite direction. We now consider the same periodically driven system but extend its period to $2T$. We use the same parametric path and redefine the period as $T'=2T$, as shown in Fig. 1(b). In this case the number of pumped charges, or $C^{\{T'\text{-}k\}}$, becomes 2. Deforming the parametric path in this new period while fixing the initial and final values of α like the ones shown in Figs. 1(c) and 1(d) does not affect the Chern number $C^{\{T'\text{-}k\}}$, which remains 2. This example illustrates the topological nature of the formulation and how the integer l naturally emerges from the extension of the old period and the redefinition of a new period. In addition, if we use the number of pumped charges during one period as a classification approach, any periodically-driven system with the same number of pumped charges within the adiabatic limit

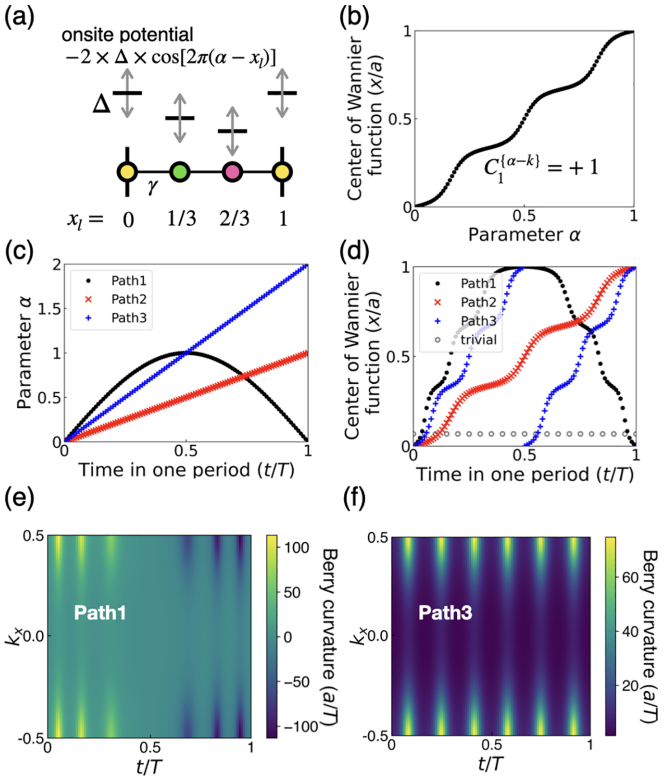

FIG. 2. Bulk 1D periodic three-site tight-binding model with a nontrivial quantum pumping. (a) The unit cell with the parameters described in the main text. (b) The evolution of the center of the Wannier function for the lowest band (labeled by 1) along a loop of the parametric variable α. The Chern number on the $\alpha - k$ plane $C_1^{\{\alpha\text{-}k\}}$ is 1. (c) Three chosen paths for $\alpha(t)$. Path1: $\alpha(t) = \sin^2(\pi t/T)$; Path2: $\alpha(t) = t/T$; Path3: $\alpha(t) = 2t/T$. (d) The evolution of the center of the Wannier function for each path within one period. For comparison, we provide a trivial case [see Eq. (3)], of which the Wannier function remains a constant, in this case, 0.07. (e) and (f) The Berry curvature on the t-k plane for Path1 ($C_1^{\{t\text{-}k\}} = 0$) and Path3 ($C_1^{\{t\text{-}k\}} = 2$), respectively.

belong to the same group. On the other hand, if we classify the system in terms of the topology hidden in the parametric function α, systems with different periodicity in the driving can still be classified as in the same class in the α-k plane.

III. RESULTS AND DISCUSSION

Here we use two 1D-spatially-periodic lattice models to demonstrate our above claims. The first example is an infinite 1D periodic tight-binding chain with three sites in a unit cell, while the second one consists of two-parallel-1D tight-binding chains described by two atoms in a unit cell. Below we use the code PythTb [25] to construct the tight-binding Hamiltonians and compute the Berry phase, Berry curvature, and Chern number. The details on the parameters for the Hamiltonians can be found below.

A. Three-site 1D tight-binding model

We use a standard 1D three-site model shown in Fig. 2(a), a simple toy model used for explaining the fundamental concepts of topology, e.g., Berry phase and Chern number, in Ref. [23]. The Hamiltonian is

$$H(\alpha) = -2\Delta \sum_i \cos[2\pi(\alpha - x_i)] c_i^\dagger c_i + \gamma \sum_i [c_{i+1}^\dagger c_i + \text{c.c.}], \quad (2)$$

where Δ is the onsite-potential amplitude, α the parametric variable to control the phase of each site, x_i the atomic position in terms of the lattice constant a, γ the coupling constant between the nearest neighbors, and $c_i(c_i^\dagger)$ the annihilation (creation) operator for an electron at site i. To make the system insulating for any α value, we use $\Delta = 2.0$ and $\gamma = -1.0$. As a result, the Hamiltonian has a nontrivial Chern number $C_n^{\{\alpha\text{-}k\}}$ for each band n. The Chern numbers for all the three bands ($n = 1$, 2, and 3) on the α-k plane $C_n^{\{\alpha\text{-}k\}}$ are 1, -2, and 1, respectively. In practice, this model can be realized, e.g., using a series of connected quantum dots, each of which is coupled to an external voltage to control the onsite potential. Here we focus on the lowest band–i.e., by considering it completely filled–but all the features and phenomena discussed below are also observed in the other bands. Figure 2(b) shows the center of the Wannier function of the lowest band as a function of α; indeed, the number of pumped charge is equal to 1, i.e., $C_1^{\{\alpha\text{-}k\}} = 1$.

We now consider the time profile of the parametric variable $\alpha(t)$. Figure 2(c) shows three arbitrary paths for $\alpha(t)$ within one T period. The paths are chosen such that the α value differs by one integer l after one period; this guarantees time periodicity in the Hamiltonian. For Path1, 2, and 3, the l values are 0, 1, and 2, respectively. The time evolution of the Wannier center for each path in one T period is shown in Fig. 2(d). If we count the number of net pumped charges at $x = 0.5a$, the number for Path1 (2, 3) is 0 (1, 2). The number is equal to the Chern number evaluated on the t-k plane, $C_n^{\{t\text{-}k\}}$.

Figures 2(e) and 2(f) show the Berry curvature on the t-k plane for Path1 and 3, respectively, within one T period. The Berry curvature for Path1 shows a symmetric feature: positive and negative values before or after $t/T = 0.5$, respectively. This is because $\alpha(t)$ returns to its original value after one period [see Fig. 2(c)] so does the corresponding center of the Wannier function [see Fig. 2(d)]. Within one T period, both Path1 and Path3 access all the possible Hamiltonians $H(\alpha)$ because of $H(\alpha + 1) = H(\alpha)$; in this case, α covers all the value in the interval [0, 1]. Interestingly, the Berry curvature and the Chern number are different for these two paths: one has a Chern number of 0, and the other 2. For Path2, the value of its Berry curvature is just half of that for Path3 with the time range [0, 0.5] and its Chern number is 1; this Berry curvature is equivalent to the Berry curvature on the α-k plane because of $\alpha(t)$=t/T. The results demonstrate that one can create a different topological invariant in the t-k space by designing how the parametric variable evolves in its own space. In addition, the Chern number on the t-k plane is exactly equal to the multiplication of the integer attached to each path and the Chern number obtained on the α-k plane. This suggests that we can use the integer l to classify a periodically-driven Hamiltonian.

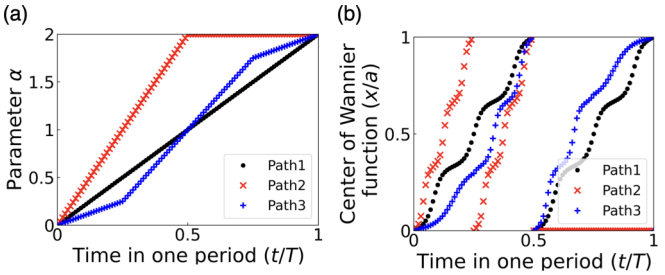

FIG. 3. Deformation of the parametric paths with the same Chern number on the t-k space. (a) Three paths with the same initial value $\alpha(t=0)=0$ and the same final value $\alpha(t=T)=2$ within one period. (b) The evolution of the center of the Wannier function for each path within one period.

Based on Eq. (1), the Chern number evaluated on the t-k plane $C_1^{\{t\text{-}k\}}$ does not change, if we deform the parametric paths by keeping the same starting and ending value within one T period. Figure 3(a) shows three possible such paths. The time evolution of the center of the Wannier function for each path is plotted in Fig. 3(b). The number of net charges passing through the unit cell, i.e., $C_1^{\{t\text{-}k\}}=2$, is indeed the same for all the chosen paths.

To compare with the above nontrivial case, we construct another similar Hamiltonian with a different onsite potential form:

$$H(\alpha) = -2\Delta\sum_i\left[\cos(2\pi\alpha)+\frac{3}{2}\left(x_i\%1-\frac{2}{3}\right)\right]c_i^\dagger c_i + \gamma\sum_i[c_{i+1}^\dagger c_i+\text{c.c.}], \tag{3}$$

where % is the modulo operator. In this case, the onsite potential of each site oscillates with the same phase and amplitude; $\Delta=0.2$ and $\gamma=-1$ are chosen to make the system have a trivial Chern number $C_n^{\{\alpha\text{-}k\}}=0$. We use the same three parametric paths $\alpha(t)$ as in the previous nontrivial case [see Fig. 2(c)] to compute the time evolution of the center of the Wannier function for the lowest band, which shows no charge pumping $C_1^{\{t\text{-}k\}}=0$ [see Fig. 2(d)]. The results from the nontrivial and trivial case imply that the Chern number $C^{\{\alpha\text{-}k\}}$ is the building block for the Chern number $C^{\{t\text{-}k\}}$.

B. Two-chains tight-binding model

The second example consists of two parallel 1D chains with the upper chain sliding with respect to the fixed lower one as shown in Fig. 4(a). This model is inspired by recent experiments where interlayer sliding has been demonstrated in van der Waals crystals and carbon nanotubes [26–28]. Compared to the previous example where the ions or sites are fixed, we demonstrate here that the formula [Eq. (1)] can also be applied to those cases where the ions are moving. The Hamiltonian with a parametric variable x_t–the x coordinate of the atom in the upper(top) chain–can be written as [29]

$$H(x_t) = \sum_{j=t,b}\delta_j\sum_i c_{j,i}^\dagger c_{j,i} + \sum_{j=t,b}\gamma_j\sum_i(c_{j,i}^\dagger c_{j,i+1}+\text{c.c.}) + \sum_{ij}\{t[r_{(t,i),(b,j)}(x_t)]c_{t,i}^\dagger c_{b,j}+\text{c.c.}\}, \tag{4}$$

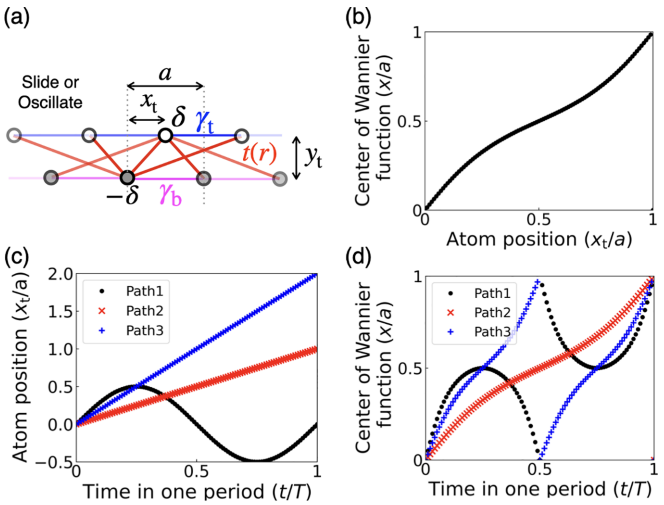

FIG. 4. Two-1D-parallel-chains tight-binding model with the upper chain sliding and the lower one fixed. (a) The unit cell is shown using the dash lines. The onsite potentials of the two atoms in the unit cell are $-\delta$ and δ, respectively. The other parameters are described in the main text. The atomic position for the lower chain in the unit cell is $(0,0)$, while that for the upper one is (x_t, y_t). (b) The evolution of the Wannier function as the upper chain moves through a unit cell. (c) The evolution of the atom position x_t for three paths. Path1: $x_t=\sin(2\pi t/T)$; Path2: $x_t=t/T$; Path3: $x_t=2t/T$. (d) The evolution of the center of the Wannier function for each path shown in (c).

where the first line describes the onsite potential and the intra-chain couplings, and the second line the interchain couplings. Here δ_j is the onsite potential for each site of the bottom (b) or top (t) chain, and γ_j the intra-chain coupling for the nearest neighbors. For the interchain coupling $t(r)$, which depends on the distance r between one atom in the bottom chain and another one in the top chain, we use $t(r)=t_{\max}e^{-(r-y_t)^2/2\sigma^2}$, where $t_{\max}$ is the maximum coupling when the atom in the upper chain is just on top of the one in the lower chain, y_t is the y coordinate of the atom in the upper chain, and σ is the effective coupling range. The distance $r_{(t,i),(b,j)}(x_t)$ can be evaluated using $\{[x_t+(j-i)a]^2+y_t^2\}^{1/2}$. Below we solve the Hamiltonian in k space, and use a σ value to consider only the coupling between the nearest sites in the upper and lower chain.

The system is set up to remain in the insulating state for any x_t value when the upper chain slides or oscillates. The parameters for the Hamiltonian are $\gamma_b=-2.0$, $\gamma_t=-0.3$, $t_{\max}=-4.0$, $\sigma=0.5$, and $\delta=0$. The evolution of the center of the Wannier function for x_t is shown in Fig. 4(b), and the number of net charges pumped within one parametric loop is 1, i.e., the Chern number for the lowest band. Notice that in this case, we do not directly compute the Chern number because of the basis change in the tight-binding model due to the movement of the upper atom in the unit cell; instead, we use the number of net pumped charges to represent the Chern number.

We choose three arbitrary paths for x_t as shown in Fig. 4(c). Path1 corresponds to the top chain oscillating around $x_t=0$. Path2 and 3 correspond to the top chain sliding with respect

to the bottom chain with a velocity of 1 and 2 (in the unit of a/T), respectively. The time evolution of the associated Wannier center for each path is shown in Fig. 4(d). Within one T period, the numbers of net pumped charges in a unit cell for Path1, 2, and 3 are 0, 1, and 2, respectively. Again, the Chern number on the t-k plane is a multiple of that on the x_t-k plane.

Here we outline a few potential future directions. Our formula [in Eq. (1)] can also be extended to include higher spatial dimensions, together with time as another dimension. In higher spatial dimensions, a periodically-driving system can have relative motions including rotation besides sliding, e.g., rotating bilayer materials [30]. Regarding experimental realizations, the list of parametric variables in a Hamiltonian is not restricted to the above two cases, onsite potentials and atomic positions; one can also choose an external time-dependent field coupled to the Hamiltonian.

IV. CONCLUSION

In summary, we have developed a general formula to show that the synthetic Chern number involving the time dimension is a multiple of another more fundamental Chern number obtained from a parametric variable α. The integer (multiple) that connects the two Chern numbers can be used to classify a periodically-driven system in the adiabatic limit. To sum up, our formula provides a tool to investigate and classify the topological properties for periodically-driven systems that can be applied within the adiabatic approximation.

ACKNOWLEDGMENTS

We acknowledge financial support from the European Research Council (Grant No. ERC-2015-AdG-694097). The Flatiron Institute is a division of the Simons Foundation. This work was supported by the Cluster of Excellence 'CUI: Advanced Imaging of Matter' of the Deutsche Forschungsgemeinschaft (DFG), EXC 2056, Grupos Consolidados (IT1453-22) and SFB925. I-T. Lu and D. Shin thank Alexander von Humboldt Foundation for the support from Humboldt Research Fellowship. J. Zhang acknowledges funding received from the European Union's Horizon 2020 research and innovation program under the Marie Sklodowska-Curie Grant Agreement No. 886291 (PeSD-NeSL). The authors thank Dr. Marios Michael, Dr. Ofer Neufeld, Dr. Shunsuke Sato, Dr. Peizhe Tang, Anatoly Obzhirov, and Osamah Sufyan for the fruitful discussion.

[1] T. Oka and S. Kitamura, Floquet engineering of quantum materials, Annu. Rev. Condens. Matter Phys. **10**, 387 (2019).
[2] U. D. Giovannini and H. Hübener, Floquet analysis of excitations in materials, J. Phys. Mater. **3**, 012001 (2020).
[3] G. E. Topp, G. Jotzu, J. W. McIver, L. Xian, A. Rubio, and M. A. Sentef, Topological Floquet engineering of twisted bilayer graphene, Phys. Rev. Res. **1**, 023031 (2019).
[4] M. S. Rudner and N. H. Lindner, Band structure engineering and non-equilibrium dynamics in Floquet topological insulators, Nat. Rev. Phys. **2**, 229 (2020).
[5] C. Weitenberg and J. Simonet, Tailoring quantum gases by Floquet engineering, Nat. Phys. **17**, 1342 (2021).
[6] M. Bukov, L. D'Alessio, and A. Polkovnikov, Universal high-frequency behavior of periodically driven systems: from dynamical stabilization to Floquet engineering, Adv. Phys. **64**, 139 (2015).
[7] M. Rodriguez-Vega, M. Vogl, and G. A. Fiete, Low-frequency and Moiré-Floquet engineering: A review, Ann. Phys. **435**, 168434 (2021).
[8] C.-M. Jian and C. Xu, Interacting Topological Insulators with Synthetic Dimensions, Phys. Rev. X **8**, 041030 (2018).
[9] M. Lohse, C. Schweizer, H. M. Price, O. Zilberberg, and I. Bloch, Exploring 4D quantum Hall physics with a 2D topological charge pump, Nature (London) **553**, 55 (2018).
[10] T. Ozawa and H. M. Price, Topological quantum matter in synthetic dimensions, Nat. Rev. Phys. **1**, 349 (2019).
[11] E. Boyers, P. J. D. Crowley, A. Chandran, and A. O. Sushkov, Exploring 2D Synthetic Quantum Hall Physics with a Quasiperiodically Driven Qubit, Phys. Rev. Lett. **125**, 160505 (2020).
[12] E. Lustig and M. Segev, Topological photonics in synthetic dimensions, Adv. Opt. Photon. **13**, 426 (2021).
[13] H. Chen, H. Zhang, Q. Wu, Y. Huang, H. Nguyen, E. Prodan, X. Zhou, and G. Huang, Creating synthetic spaces for higher-order topological sound transport, Nat. Commun. **12**, 5028 (2021).
[14] I. Martin, G. Refael, and B. Halperin, Topological Frequency Conversion in Strongly Driven Quantum Systems, Phys. Rev. X **7**, 041008 (2017).
[15] Y. Baum and G. Refael, Setting Boundaries with Memory: Generation of Topological Boundary States in Floquet-Induced Synthetic Crystals, Phys. Rev. Lett. **120**, 106402 (2018).
[16] Y. Peng and G. Refael, Topological energy conversion through the bulk or the boundary of driven systems, Phys. Rev. B **97**, 134303 (2018).
[17] P. J. D. Crowley, I. Martin, and A. Chandran, Topological classification of quasiperiodically driven quantum systems, Phys. Rev. B **99**, 064306 (2019).
[18] Z. Qi, G. Refael, and Y. Peng, Universal nonadiabatic energy pumping in a quasiperiodically driven extended system, Phys. Rev. B **104**, 224301 (2021).
[19] S. Nakajima, T. Tomita, S. Taie, T. Ichinose, H. Ozawa, L. Wang, M. Troyer, and Y. Takahashi, Topological Thouless pumping of ultracold fermions, Nat. Phys. **12**, 296 (2016).
[20] D. J. Thouless, Quantization of particle transport, Phys. Rev. B **27**, 6083 (1983).
[21] M. Lohse, C. Schweizer, O. Zilberberg, M. Aidelsburger, and I. Bloch, A Thouless quantum pump with ultracold bosonic atoms in an optical superlattice, Nat. Phys. **12**, 350 (2016).
[22] W. Ma, L. Zhou, Q. Zhang, M. Li, C. Cheng, J. Geng, X. Rong, F. Shi, J. Gong, and J. Du, Experimental Observation of a Generalized Thouless Pump with a Single Spin, Phys. Rev. Lett. **120**, 120501 (2018).

[23] D. Vanderbilt, *Berry Phases in Electronic Structure Theory: Electric Polarization, Orbital Magnetization and Topological Insulators* (Cambridge University Press, 2018).

[24] The Chern number on the $t - k$ plane can be determined from that on the $\alpha - k$ plane in the adiabatic limit; therefore, we say the latter is more fundamental.

[25] PythTB official website, http://physics.rutgers.edu/pythtb/.

[26] M. Vizner Stern, Y. Waschitz, W. Cao, I. Nevo, K. Watanabe, T. Taniguchi, E. Sela, M. Urbakh, O. Hod, and M. Ben Shalom, Interfacial ferroelectricity by van der Waals sliding, Science **372**, 1462 (2021).

[27] M. Wu and J. Li, Sliding ferroelectricity in 2D van der Waals materials: Related physics and future opportunities, Proc. Natl. Acad. Sci. USA **118**, e2115703118 (2021).

[28] J. Cumings and A. Zettl, Low-friction nanoscale linear bearing realized from multiwall carbon nanotubes, Science **289**, 602 (2000).

[29] The two-1D-sliding-chains model includes the possibility of inducing a topological phase transition through parametric sliding. Here we focus on one insulating phase without gap closure during sliding.

[30] J.-Z. Ma, T. Datta, and D.-X. Yao, Effective curved space-time geometric theory of generic-twist-angle graphene with application to a rotating bilayer configuration, Phys. Rev. B **105**, 245102 (2022).